Simulation of High-Q Nanocavities with 1D Photonic Gap

Jiří Petráček[1], Bjorn Maes[2], Sven Burger[3], Jaroslav Luksch[1], Pavel Kwiecien[4], Ivan Richter[4]

[1] *Institute of Physical Engineering, Brno University of Technology*
Technická 2, CZ-616 69 Brno, Czech Republic

[2] *Micro- and Nanophotonic Materials Group, University of Mons, Faculty of Science,*
Avenue Maistriau 19, B-7000 Mons, Belgium

[3] *Zuse Institute Berlin (ZIB), Takustraße 7, D–14 195 Berlin, Germany*

[4] *Department of Physical Electronics, Faculty of Nuclear Sciences and Physical Engineering, Czech Technical University in Prague, Břehová 7, 115 19 Praha 1, Czech Republic*

Tel: +420 541 142 764, Fax: +420 541 142 842, e-mail: petracek@fme.vutbr.cz

ABSTRACT

We report on theoretical investigation of a hybrid cavity structure which has been conducted within the European Action COST MP0702. The structure, which can reach ultrahigh Q factors, consists of a size-modulated 1D stack cavity made in a III-V material and coupled to a silicon waveguide. We present results of structure behavior simulations obtained by four independent rigorous numerical techniques. We discuss qualitative physical properties of the simulations results and identify the main physical effects contributing to the total Q factor.

Keywords: high-Q nanocavity, photonic crystals, resonant frequency, numerical modeling, bidirectional mode expansion and propagation method, finite difference time domain method, finite element method, rigorous coupled wave analysis

1. INTRODUCTION

Optical nanocavities with high-quality factors (Q) and small modal volumes have become useful in nanophotonics for a wide range of important applications, such as miniature sensors and filters, low-threshold lasers, and low-power optical switches. The research has been mainly concentrated on structures with 2D or 3D photonic band gaps. Recently, however, cavities in size-modulated 1D periodic structures with 1D photonic gaps were studied too; it was shown that they could reach ultrahigh values of Q factor while maintaining wavelength-sized dimensions [1]. These size-modulated 1D cavities exhibit simple geometry which opens new potential for wavelength-scale, high-quality cavity devices. We consequently employed this cavity structure as the basis for a practical modeling exercise, originally under the umbrella of COST MP0702 Action, with the added value of studying hybrid material device physics.

The investigated structure, which is illustrated in Fig. 1, consists of the size-modulated 1D cavity coupled to an (input or output) straight waveguide. The cavity is made in a III-V material (InP is proposed here), as such materials are effective for active components. The waveguide is considered in silicon, which has been proven as a suitable base for integrated waveguide devices.

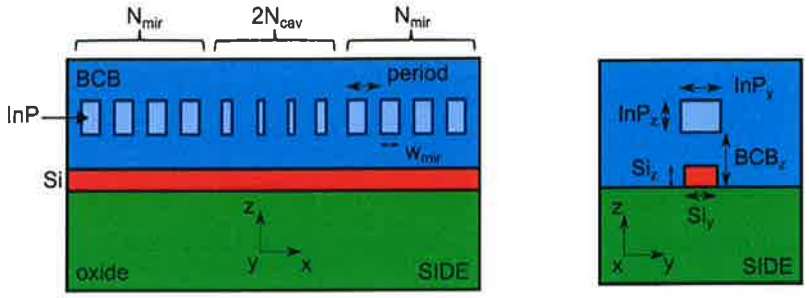

Figure 1. Geometry of the size-modulated 1D hybrid cavity coupled to the waveguide. The cavity is formed with the InP sections (veins), the Si waveguide functions as the input/output coupler. The widths of $2N_{cav}$ veins are modulated so that the thinnest veins are located near cavity centre.

In this work, we briefly report on simulations of this hybrid cavity structure using four independent rigorous numerical techniques. We discuss qualitative physical properties of the simulations results and identify the main physical effects contributing to the total Q factor. Note, however, that the proposal of the structure and the full results of the study will be published elsewhere [2].

2. NUMERICAL TECHNIQUES

Clearly, simulation of resonant 3D structures demands very efficient and reliable computational methods. In our study, we used the following approaches:

- Bidirectional eigenmode propagation (BEP) is a modal expansion scheme. The waveguide modes are searched by means of the finite-element commercially available software COMSOL Multiphysics. (Modes of homogeneous sections are calculated analytically.) The technique was effectively combined with the propagation algorithm of numerically-stable scattering matrices where the interface matrices were determined from the overlap integrals of modal fields [3]. Resonance wavelength and Q factor have been calculated from eigenvalues of the reflectivity matrix [4]. Note that this algorithm has been found to provide more reliable results than the standard approach based on locating of the maximum and bandwidth of a resonance curve.
- The finite-difference time-domain (FDTD) method, using the freely available software package MEEP [5].
- The time-harmonic, higher-order 3D finite element (FE) solver JCMsuite with adaptive meshing; it has been used to compute resonance modes and corresponding complex eigenfrequencies of the cavity directly [6]. Afterwards, from the complex eigenvalues, resonance wavelength and Q factor have been derived [7].
- Aperiodic rigorous coupled wave analysis (aRCWA); it is the Fourier expansion scheme which uses in-house robust 3D tool effectively combining both 2D mode solver (based on 2D periodic RCWA tool in a combination with the isolating boundary conditions of a PML type, in the form of either complex coordinate transforms or anisotropic layers [8,9]), with the help of both ASR technique [10] and/or the application of structural symmetries [11], and the advanced "grating-oriented" schemes of scattering matrix formalism. Resonance wavelengths and Q factors have been calculated with the same procedure as in the case of the BEP technique described above.

3. RESULTS

Referring to Fig. 1, we used the following parameters for the calculation: $InP_y = 0.7$ μm, $InP_z = 0.35$ μm, $Si_z = 0.22$ μm and $BCB_z = 1.0$ μm. Refractive indices in materials used within the structure were chosen as 3.46 (Si), 1.45 (silicon oxide), 3.17 (InP) and 1.54 (benzocyclobuten-based polymer, BCB).

Center positions of the InP sections (veins) were regularly spaced with the period $a = 0.35$ μm. The number of modulated veins on each side of the cavity center were marked as N_{cav}. Here we considered modulation of the vein widths given by the formula:

$$w(i) = (0.15\,\mu\text{m})\left[1 + \frac{(i-1)^2}{3N_{cav}^2}\right], \quad i = 1...N_{cav} \tag{1}$$

Both cavity "mirrors" are formed by N_{mir} veins, $N_{mir} = 10$, with constant width $w_{mir} = 0.2$ μm.

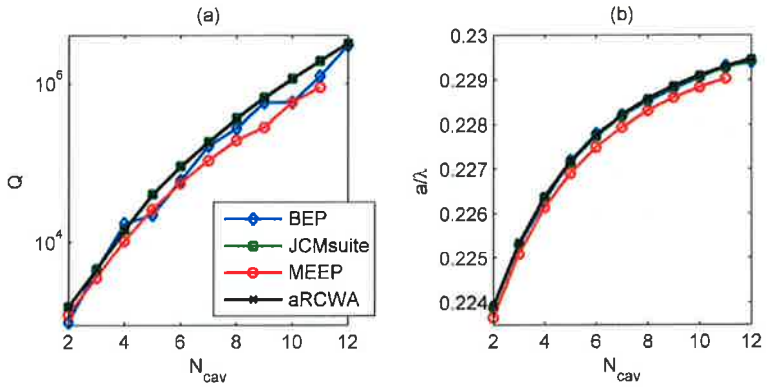

Figure 2. Simulation results for the single cavity. (a) Quality factor Q and (b) normalized resonance frequency a/λ versus N_{cav} calculated by the four numerical techniques (BEP - blue diamonds, JCMsuite - green squares, MEEP - red circles, aRCWA – black crosses).

We first present results for a single cavity when there are no waveguide and no substrate nearby present. Figures 2 (a) and (b) show Q and the normalized resonance frequency a/λ (λ is the resonance wavelength) of the fundamental quasi-TE cavity mode (electric field parallel with y axis). Accordingly, the results and the principle of cavity operation can be explained with the help of Fig. 3 as follows [2]. Let us start first with the periodic 1D stack structure (no vein modulation) which can support Bloch modes. Indeed, position of the bandgap strongly depends on the widths of the veins. Consider, for example, operating frequency shown by horizontal blue line in Fig. 3 and allow modulation of vein widths with the aim to create the size-modulated cavity. The modulation is

chosen so that the Bloch mode is propagating in the center of the cavity (veins with width w = 0.15 μm) and evanescent in the mirror sections on the cavity sides ($w = w_{mir}$ = 0.2 μm). Thus the mode, which was propagating in the center, can be scattered into radiation or reflected in the mirror sections. The radiation, however, can be significantly suppressed by slow change of vein thicknesses, *i.e.* when N_{cav} is increased. In this way, it is possible to achieve very high reflections, and consequently cavity modes with high Q.

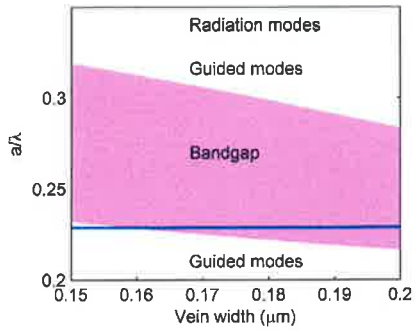

Figure 3. Gradual shift of the bandgap for the periodic 1D stack structure. The horizontal blue line indicates the resonance frequency for the size-modulated 1D cavity with N_{cav} = 10; the results were calculated using the BEP technique.

The radiation suppression which results in the strong increase of Q is clearly seen in Fig. 2(a). As N_{cav} increases, the rate of increase of Q lessens gradually. Thus for small N_{cav}, the structure is quite sensitive to increasing N_{cav}, leading to a rapid decline of radiation losses and increasing Q. At higher N_{cav}, a slightly slower exponential increase is seen. We observed that, in this regime, the losses mainly depend on the number of mirror veins N_{mir}, similarly as for reflections from the Bragg mirror.

As shown in Fig. 2(b), the normalized resonance frequency increases slightly as a function of N_{cav} and saturates close to the upper limit of the Bloch mode frequency in the center of the cavity. This is because there are standing waves present in the cavity at the resonance. For perfectly periodic structure (no width modulation), this is only possible at the edge of the Brillouin zone. Therefore, with increasing N_{cav} the guided Bloch mode in cavity centre approaches the edge of the Brillouin zone and consequently the frequency is limited by the band maximum.

Presence of a Si waveguide can significantly change the cavity performance. In this case coupling between the cavity and the waveguide may cause additional losses and affect the total quality factor. Therefore change in Q depends strongly on the waveguide properties. As an example, Fig. 4 shows the influence of the Si waveguide width Si_y for various constant values of N_{cav}. We observe that Q exhibits a dip around a certain value of Si_y = 0.33 μm. This behavior can be understood by considering coupling between the waveguide and cavity mode. To support our argument, Fig. 5 shows effective indices of these modes for a/λ = 0.229, as a function of the waveguide width Si_y; indeed the effective index of the waveguide mode varies accordingly with this width. It is seen that, at the width of Si_y = 0.33 μm, one obtains phase matching between the modes [2], leading to a strong coupling, just as in conventional directional couplers.

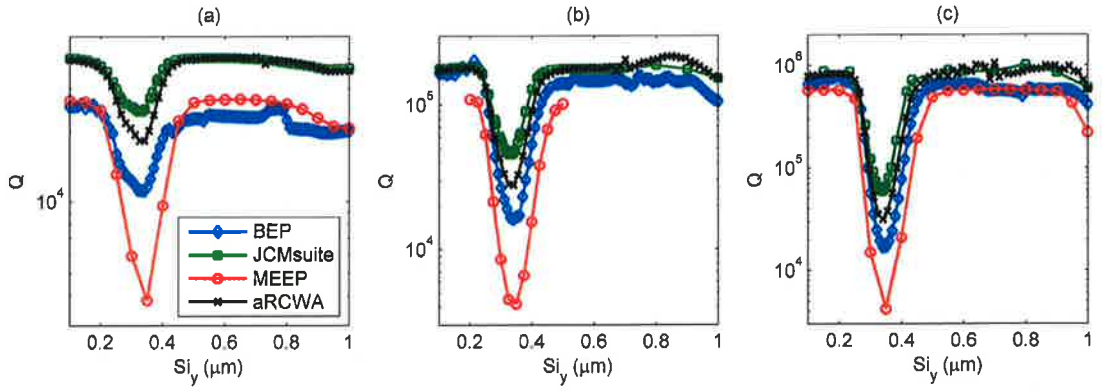

Figure 4. Simulation results calculated by the four numerical techniques for the cavity coupled to the waveguide. Quality factor Q versus Si waveguide width Si_y, for (a) N_{cav} = 5, (b) N_{cav} = 7, and (c) N_{cav} = 10.

Considering comparison of the four numerical methods, we observe reasonably good agreement in Fig. 2. Note, however, that deviations of the BEP results around the central smooth trend in Fig. 2(a) (and also small

oscillations seen in Fig. 4) are probably numerical artefacts caused by imperfect boundary conditions. Similarly, the effectiveness of transparent boundary conditions (represented with perfectly matched layers) can influence the results and cause small quantitative differences, such as observed in Fig. 2. For FE (JCMsuite) we have checked that PML settings are chosen such that the influence of artificial reflections is negligible.

In Fig. 4 the techniques provide good qualitative agreement. However, there are significant differences in quantitative results. This is because small errors, which are inevitable in any numerical technique, are amplified by resonant behavior of the simulated device.

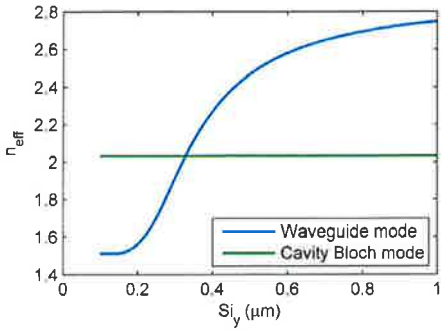

Figure 5. The phase matching between the waveguide mode and the central cavity mode. The graph shows effective indices n_{eff} of the Si waveguide mode (as a function of width Si_y) and the Bloch mode in the cavity centre. The results were calculated for $a/\lambda = 0.229$.

4. CONCLUSIONS

The four rigorous numerical techniques have been applied to the novel and promising structure, the high-Q size-modulated 1D nanocavity. The all techniques have appeared efficient in providing the important cavity characteristics, with their advantages and disadvantages. It has been shown that the coupling between the cavity and the waveguide is due to a sensitive phase-matching process, which needs to be controlled to achieve an optimum design. Quantitative differences among numerical results demonstrate that accurate computation of 3D resonators still remains a challenging problem which should be further investigated.

ACKNOWLEDGEMENTS

The work was conducted within the European Action COST MP0702. J.P., J.L, P.K. and I.R. acknowledge the support of this work by Czech Science Foundation under the contract P205/10/0046, P.K. and I.R also the Ministry of Education, Youth and Sports of the CR project OC09038. B.M. acknowledges the Stevin Supercomputer Infrastructure at Ghent University, funded by Ghent University, the Hercules Foundation and the Flemish Government department EWI.

REFERENCES

[1] M. Notomi, E. Kuramochi, H. Taniyama: Ultrahigh-Q nanocavity with 1D photonic gap, *Opt. Express*, vol. 16, no. 15, pp. 11059-11102, Jul. 2008.

[2] B. Maes, *et al.*: Numerical method comparison for high-Q optical nanocavities. To be published.

[3] P. Bienstman, R. Baets: Optical modelling of photonic crystals and VCSELs using eigenmode expansion and perfectly matched layers, *Opt. Quantum Electron.*, vol. 33, no. 4-5, pp. 327-341, Apr. 2001.

[4] N. Gregersen, *et al.*: Numerical and experimental study of the Q factor of high-Q micropillar cavities, *IEEE J. Quantum Electron.* vol. 46, no. 10, pp. 1470-1483, Oct. 2010.

[5] A. F. Oskooi, *et al.*: MEEP: A flexible free-software package for electromagnetic simulations by the FDTD method, *Comp. Phys. Commun.* vol. 181, no. 3, pp. 687–702, Mar. 2010.

[6] J. Pomplun, *et al.*: Adaptive finite element method for simulation of optical nano structures, *Phys. Stat. Sol. (b)*, vol. 244, no. 10, pp. 3419-3434, Oct. 2007.

[7] S. Burger, *et al.*: Finite-element method simulations of high-Q nanocavities with 1D photonic bandgap, *Proc. SPIE*, vol. 7933, p. 79330T, Jan. 2011.

[8] E. Silberstein, *et al.*: Use of grating theories in integrated optics, *JOSA A*, vol. 18, no. 11, pp. 2865-2875, Nov. 2001.

[9] J.-P. Hugonin, P. Lalanne: Perfectly matched layers as nonlinear coordinate transforms: A generalized formalization, *JOSA A*, vol. 22, no. 9, pp. 1844-1849, Sep. 2001.

[10] J. Čtyroký, P. Kwiecien, I. Richter: Fourier series-based bidirectional propagation algorithm with adaptive spatial resolution, *J. Lightwave Technol.*, vol. 28, no. 20, pp. 2969-2976, Oct. 2010.

[11] Z.Y. Li, K.M. Ho: Application of structural symmetries in the plane-wave-based transfer-matrix method for three-dimensional photonic crystal waveguides, *Phys. Rev. B*, vol. 68, no. 24, pp. 245117-1-20, Dec. 2003.